SCIENTIFIC REP🅞RTS

OPEN

Identifying the origin of nitrous oxide dissolved in deep ocean by concentration and isotopocule analyses

Sakae Toyoda [1], Osamu Yoshida[2], Hiroaki Yamagishi[3,6], Ayako Fujii[3,7], Naohiro Yoshida [1,4] & Shuichi Watanabe[5]

Nitrous oxide (N_2O) contributes to global warming and stratospheric ozone depletion. Although its major sources are regarded as bacterial or archaeal nitrification and denitrification in soil and water, the origins of ubiquitous marine N_2O maximum at depths of 100–800 m and N_2O dissolved in deeper seawater have not been identified. We examined N_2O production processes in the middle and deep sea by analyzing vertical profiles of N_2O concentration and isotopocule ratios, abundance ratios of molecules substituted with rare stable isotopes ^{15}N or ^{18}O to common molecules $^{14}N^{14}N^{16}O$, in the Atlantic, Pacific, Indian, and Southern oceans. Isotopocule ratios suggest that the N_2O concentration maxima is generated by *in situ* microbial processes rather than lateral advection or diffusion from biologically active sea areas such as the eastern tropical North Pacific. Major production process is nitrification by ammonia-oxidizing archaea (AOA) in the North Pacific although other processes such as bacterial nitrification/denitrification and nitrifier-denitrification also significantly contribute in the equatorial Pacific, eastern South Pacific, Southern Ocean/southeastern Indian Ocean, and tropical South Atlantic. Concentrations of N_2O below 2000 m show significant correlation with the water mass age, which supports an earlier report suggesting production of N_2O during deep water circulation. Furthermore, the isotopocule ratios suggest that AOA produce N_2O in deep waters. These facts indicate that AOA have a more important role in marine N_2O production than bacteria and that change in global deep water circulation could affect concentration and isotopocule ratios of atmospheric N_2O in a millennium time scale.

The oceans are estimated as the third largest source of atmospheric N_2O after natural soil and agriculture[1]. Oceans are also a large reservoir of this greenhouse and ozone-depleting gas because N_2O has seawater solubility as high as CO_2[2]. Moreover, oversaturation of N_2O is often found at depths below the surface layer (<ca. 100 m depth)[3]. In many ocean areas, the N_2O concentration increases with depth and shows a maximum at 100–800 m depth. The highest concentration is found in the eastern tropical North/South Pacific (ETNP/ETSP)[4]. Based on these facts, it has been proposed that N_2O produced in the ETNP/ETSP, where biological activities are very high because of upwelling of nutrient rich water, is globally transported by isopycnal movement of seawater[4]. However, one earlier report describes that N_2O concentrations in the water deeper than 2000 m show positive correlation with the age of the water with respect to global circulation[5], suggesting that N_2O production might also occur in the deep water. Although deep waters do not contact with the atmosphere, such N_2O oversaturation is expected to affect ocean-to-atmosphere flux of N_2O on a longer time scale by diffusive transport or by change in global ocean

[1]Department of Chemical Science and Engineering, School of Materials and Chemical Technology, Tokyo Institute of Technology, Yokohama, Japan. [2]College of Agriculture, Food and Environment Sciences, Rakuno Gakuen University, Ebetsu, Hokkaido, Japan. [3]Interdisciplinary Graduate School of Science and Engineering, Tokyo Institute of Technology, Yokohama, Japan. [4]Earth-Life Science Institute, Tokyo Institute of Technology, Tokyo, Japan. [5]Mutsu Institute for Oceanography, Japan Agency for Marine-Earth Science and Technology, Mutsu, Aomori, Japan. [6]Present address: Environmental Health Department, Ministry of the Environment, Tokyo, Japan. [7]Present address: Tokyo University of Agriculture, Tokyo, Japan. Correspondence and requests for materials should be addressed to S.T. (email: toyoda.s.aa@m.titech.ac.jp)
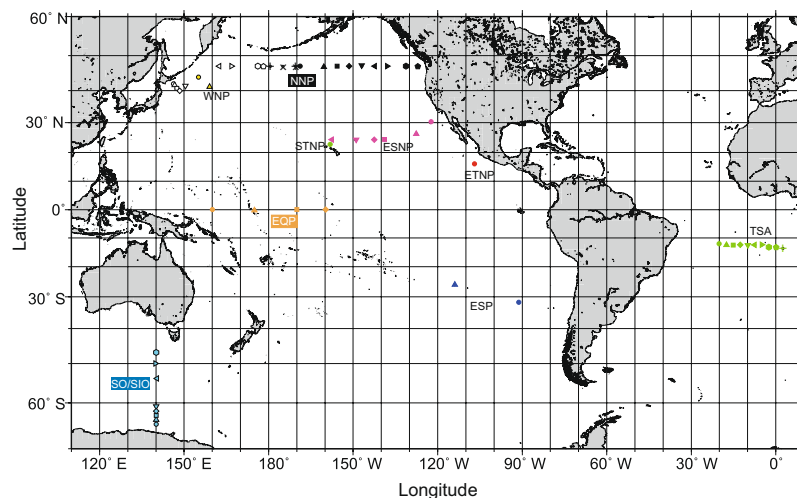
Figure 1. Map showing seawater sampling stations. In this work, observations in the northern North Pacific (NNP), equatorial Pacific (EQP), and Southern Ocean/southeastern Indian Ocean (SO/SIO) were conducted. Data in other regions were compiled from previous studies. See also Table S1. Each symbol corresponds to the symbol presented in Figs 2 and 3.

circulation. Nevertheless, the origin and production mechanisms of the N_2O maximum and the N_2O in deep water remain uncertain.

Isotopocule ratios ($\delta^{15}N$, $\delta^{18}O$, and SP, ^{15}N-site preference in NNO molecule) of N_2O are useful parameters to identify the origin and production–consumption processes of N_2O because they depend on the isotopic ratios in precursors and isotope effects of chemical or biochemical reactions[6]. Reportedly, the magnitudes of isotope effects on nitrogen during N_2O production as byproduct of nitrification by ammonia oxidizing bacteria (AOB)[7,8] and ammonia oxidizing archaea (AOA)[9,10] differ. Moreover, SP values of N_2O produced by AOB via hydroxylamine (NH_2OH)[9,11] and by AOA[9,10,12] are distinct from the values of N_2O produced by AOB via nitrite (NO_2^-)[8,11,13,14] or by denitrification[11,15] (Supplementary Fig. S1, Table S2). When N_2O is partially reduced to N_2 in denitrification, all isotopocule ratios increase[16–20]. Although the isotope effect during N_2O reduction varies among bacterial species or pure culture and community incubations, consistent relations have been found between isotope effects on N, O, and SP[16].

Several earlier studies have analyzed vertical profiles of concentration and isotopocule ratios of N_2O in the ocean and have investigated production–consumption processes specific to the depths or sites[17,21–25]. Nevertheless, it remains unclear whether N_2O is produced *in situ* or transported from other regions because existing data do not cover the wide range of oceanic setting such as circulation age of deep seawater. This report describes new isotopocule analyses of N_2O in the northern North Pacific (NNP), equatorial Pacific (EQP), and Southern Ocean and southeastern Indian Ocean (SO/SIO) where younger, medium, and older water respectively exist in deep layers (Fig. 1). The respective results are compared with existing observations to ascertain the origin of N_2O from the perspective of global deep water circulation.

Vertical Profiles of Dissolved N_2O

In the surface layer, concentrations of N_2O measured in the eight regions except the eastern tropical North Pacific (ETNP) are as low as those expected under the dissolution equilibrium between atmosphere and seawater (6–8 nmol kg^{-1}). However, they increase with depth and reach a maximum (25–65 nmol kg^{-1}) (Fig. 2a). The depth of the maximum is 100–400 m in the tropical South Atlantic (TSA), SO, and EQP, and 400–1500 m in other regions. Those values correspond to almost identical seawater density (potential density anomaly, σ_θ, of about 27) (Supplementary Table S1). Below the maximum, the N_2O concentration decreases with depth. It reaches 15–40 nmol kg^{-1} in the deep layer (>2000 m depth or $\sigma_\theta = 27.7$–27.8). In the ETNP, two concentration maxima exist at 60 m ($\sigma_\theta = 25.0$) and 800 m ($\sigma_\theta = 27.3$)[17].

Each of the three independent isotopocule ratios shows a unique profile that is different from that of concentration (Fig. 2b–d). The bulk (or average) nitrogen isotope ratio ($\delta^{15}N^{bulk}$) in the eight regions except ETNP shows no vertical gradient from the surface to the depth corresponding to $\sigma_\theta \cong 25$. Then it decreases slightly with depth, showing a minimum value at $\sigma_\theta \cong 26$. Below the small minimum, it increases monotonically with depth and reaches its maximum (9–10‰) at the bottom layer. In the ETNP, it shows a minimum and a maximum respectively corresponding to the shallow and deep concentration maxima. The oxygen isotope ratio ($\delta^{18}O$) and ^{15}N-site preference (SP) also show almost constant values from the surface to the depth above the concentration maximum ($\sigma_\theta \cong 26$) in the eight regions. In deeper water, however, their vertical profiles are markedly different among oceanic regions. Although $\delta^{18}O$ and SP respectively show a parallel increase and decrease with concentration in the North Pacific stations, they exhibit a monotonic increase in EQP, SO/SIO, and ESP. In TSA, they show minima at the concentration maximum.
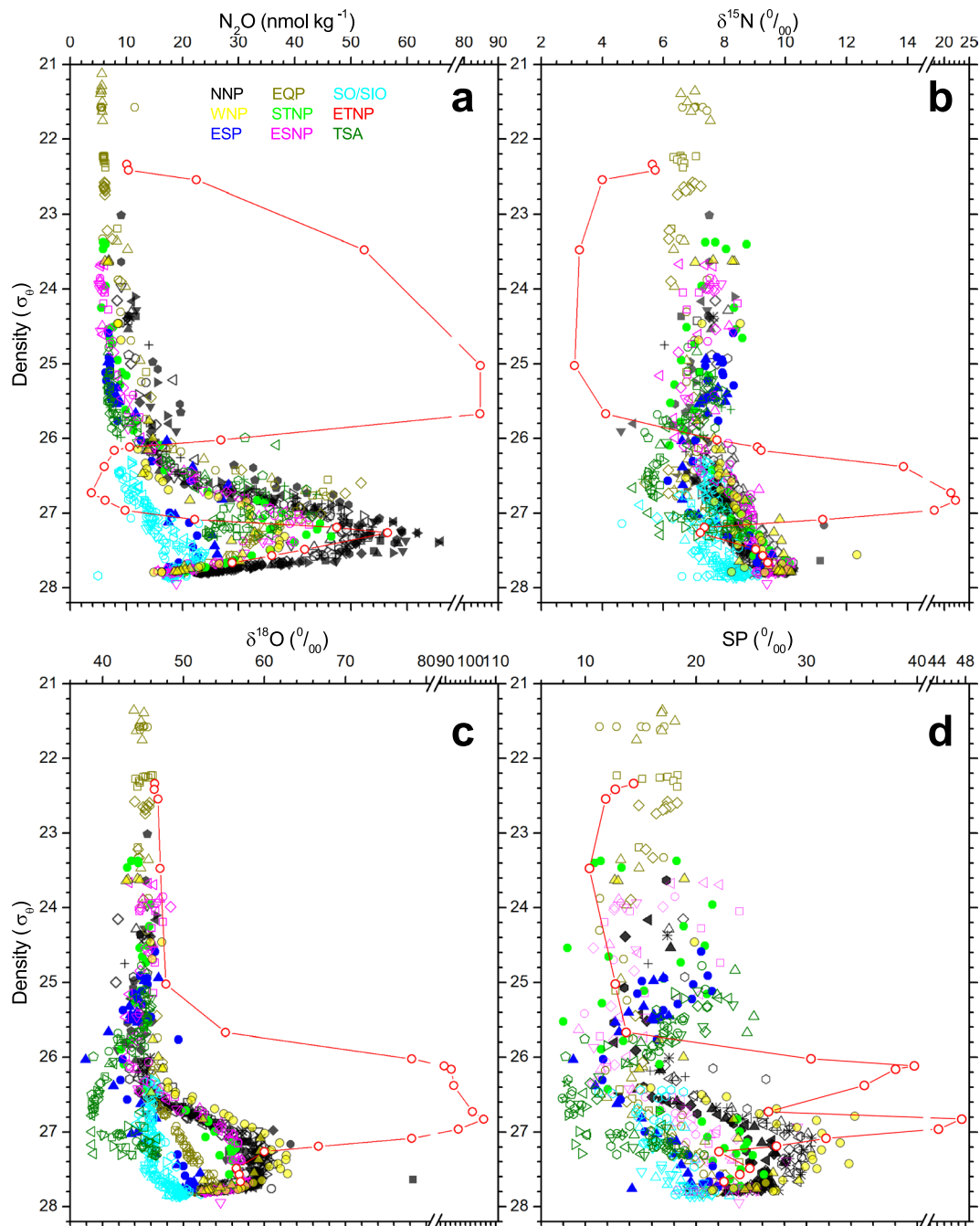
Figure 2. Vertical distribution of concentrations and isotopocule ratios of N_2O in nine oceanic regions. (**a–d**) Concentration (**a**), $\delta^{15}N^{bulk}$ (**b**), $\delta^{18}O$ (**c**), and SP (**d**). Symbol colors represent regions. Vertical axis shows potential density anomaly instead of depth, in order to compare the N_2O profiles obtained from regions with different physical structures. When samples were collected at several stations in a region, the symbol type was changed accordingly: NNP, northern North Pacific; EQP, equatorial Pacific; SO/SIO, Southern Ocean/ southeastern Indian Ocean; WNP, western North Pacific; STNP, subtropical North Pacific; ETNP, eastern tropical North Pacific; ESP, eastern South Pacific; ESNP, eastern subtropical North Pacific; TSA, tropical South Atlantic. See Table S1 for data sources.

Origin of N_2O at Concentration Maximum

Isotopic signatures of N_2O at density level of $\sigma_\theta = 27.3$ which corresponds to concentration maximum in ETNP show systematic difference between oceanic regions (Fig. 3). For example, in spite of similarity in water mass property (temperature and salinity, data not shown) between NNP and WNP and between EQP and ETNP, they are distinguished each other. Variations of isotopocule ratios are caused by (1) mixing of N_2O with different isotopic signatures such as N_2O produced *in situ*, advected from other regions, and dissolved atmospheric N_2O or (2) decomposition of N_2O during which the remaining N_2O is isotopically fractionated[6]. Based on a global
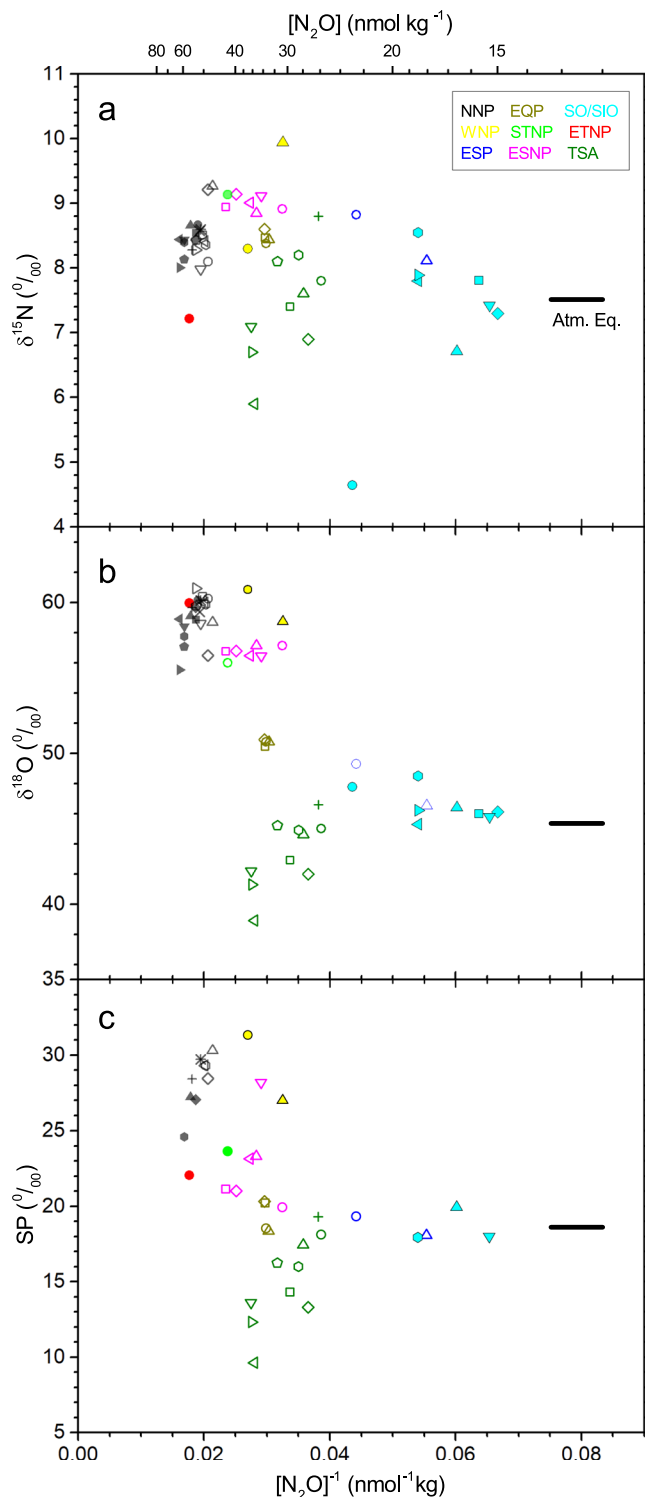
Figure 3. Comparison of isotopocule ratios of N_2O at concentration maximum in nine oceanic regions. (**a**–**c**) Relations between inverse concentration and $\delta^{15}N^{bulk}$ (**a**), $\delta^{18}O$ (**b**), and SP (**c**). Colors and types of symbols are as shown in Fig. 2. Horizontal solid lines show values of dissolved N_2O when the seawater is equilibrated with the atmosphere.

distribution of N_2O concentration, it has been proposed that N_2O produced in the eastern tropical Pacific is exported to other regions in the Pacific by lateral or isopycnal advection[4]. If this is the case, and if we consider mixing of two endmembers, namely, N_2O produced in the ETNP and background N_2O from the atmosphere, the isotopic data points for the regions outside the ETNP is expected to fall on the mixing line in isotope–reciprocal concentration plot. However, the results show that mixing between N_2O in the ETNP and N_2O in the water equilibrated with the atmosphere cannot explain the observed isotopocule ratios in the eight regions (Fig. 3). In
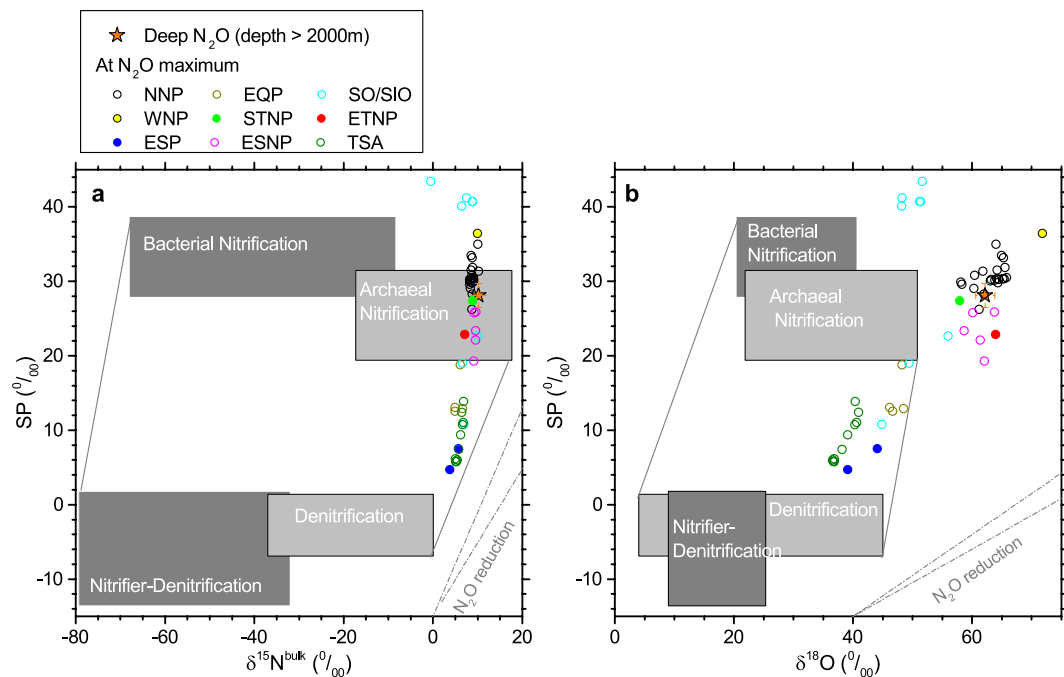
Figure 4. Comparison of isotopocule ratio of the excess N_2O produced at concentration maximum (circles) and deeper seawater (orange star). (**a,b**) Relation between $\delta^{15}N^{bulk}$ and SP (**a**) and the relation between $\delta^{18}O$ and SP (**b**). Rectangles respectively show ranges expected when N_2O is produced by the indicated microbial processes (See Supplementary Information). Broken lines show range of the slope expected for increase in isotopocule ratios during partial reduction by denitrification.

other words, the isotopocule ratios for excess N_2O at N_2O maxima in the eight regions, as calculated assuming isotopic mass balance between observed and background N_2O, are distinct from those obtained at ETNP (Fig. 4 and Table S1).

In Fig. 3, N_2O maxima in NNP could be regarded as an alternative endmember because of its high concentration. However, lateral advection of N_2O from NNP is also improbable for the following reasons. First, the distribution of data obtained in other regions still cannot be explained consistently by the isopycnal mixing in each panel of Fig. 3. Second, vertical profiles of temperature and salinity at the stations in this work do not show discontinuous feature which is expected if different water mass is advected laterally.

Contribution from partial reduction of N_2O (the second factor noted above) is also unlikely because all the isotopic signatures should be increased with decreasing concentration and because nitrate reduction, which is the first step of denitrification and prerequisite for N_2O reduction, is not prominent in the observed oxic water columns. Therefore, we infer that the N_2O maximum is a result of *in situ* production rather than advection from other regions. Possible production mechanisms are discussed below together with those for deep water N_2O.

Origin of N_2O in Deep Layer

The concentration of N_2O averaged for water below 2000 m depth shows a positive correlation with the circulation age of seawater estimated from the ^{14}C content[26] (Fig. 5a). Bange and Andreae found a similar relation by compiling 56 observations from the North/South Atlantic, North/South Indian, and North Pacific oceans[5]. Based on insignificant fluxes estimated for hydrothermal or sediment N_2O, they concluded that N_2O is produced in the deep ocean mainly by nitrification. The slope of the regression line in Fig. 5a ($(1.0 \pm 0.2) \times 10^{-2}$ nmol kg^{-1} yr^{-1}) is comparable to their reported value of $(5.7 \pm 1.0) \times 10^{-3}$ nmol L^{-1} yr^{-1} and the y-intercept (14.3 ± 2.2 nmol kg^{-1}) agrees with the earlier report (13.1 nmol kg^{-1})[5]. Here we show that isotopocule ratios also increase with the circulation age. When plotted against inverse N_2O concentration, they are distributed on a line that passes ranges of surface water that is saturated with the atmosphere (Fig. 5b). This confirms that N_2O is added during the circulation of deep seawater after losing contact with the atmosphere, and the following isotopocule ratios of the produced N_2O are obtained as y-intercepts of the regression lines: 10.2 ± 0.4‰, 62.2 ± 1.6‰, and 28.1 ± 1.6‰, respectively, for $\delta^{15}N^{bulk}$, $\delta^{18}O$, and SP.

A closer look at Fig. 5a and Supplementary Table S1 reveals systematic difference in N_2O concentration between NNP, STNP, WNP, and ESNP. Since it has been suggested that deep water circulates from the South Pacific to these north Pacific regions via different routes[27,28], N_2O production rate during the circulation might vary with the pathways. For instance, dissolved oxygen concentration in the deep layer is lowest in NNP[29], which could explain the higher N_2O concentration in NNP than other North Pacific regions because N_2O production is enhanced under low oxygen condition[12,30]. Additional factor that could partly explain the positive deviations of NNP data from the fitted line is underestimation of age for the NNP waters (Matsumoto, personal communication).
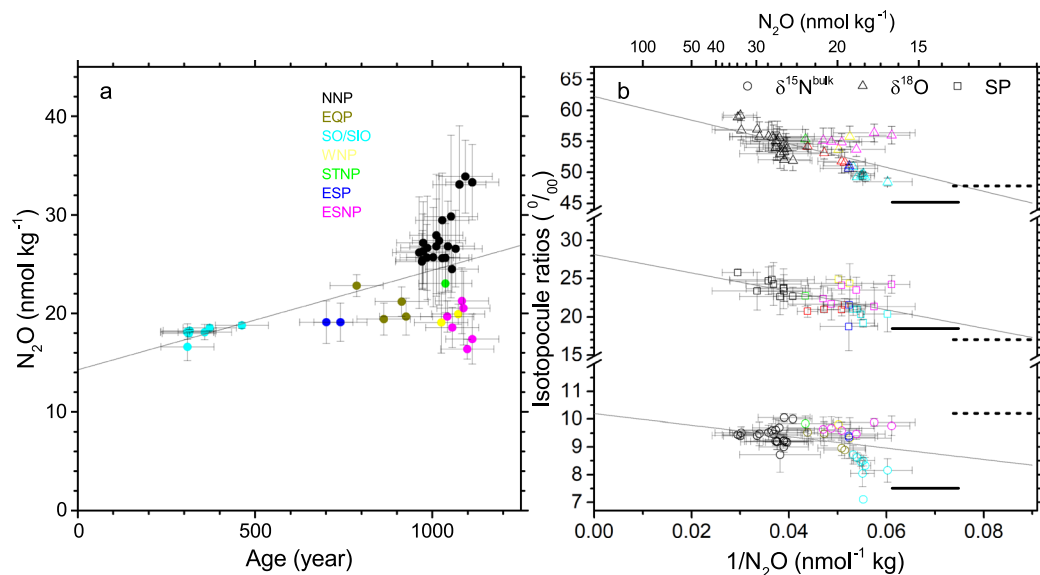
Figure 5. Concentration and isotopocule ratios of N_2O for deep water (depth >2000 m) in nine oceanic regions and their relation with circulation age of seawater. (**a,b**) Relation between circulation age and N_2O concentration (**a**) and relation between iverse concentration and isotopocule ratios of N_2O (**b**). Each symbol denotes the average for the deep water at each station. Error bars for concentration and isotopocule ratios show one standard deviation while those for age are reported estimated error[26]. Solid and broken horizontal lines in panel b respectively show the values expected when the surface water in the subduction region is equilibrated with modern and preindustrial atmosphere[31]. Correlation coefficients of regression lines and probabilities of null hypothesis in ANOVA are as follows. In panel a, $r = 0.55$, $p = 1.3 \times 10^{-4}$; in panel b, $\delta^{15}N^{bulk}$, $r = -0.38$, $p = 1.3 \times 10^{-2}$; $\delta^{18}O$, $r = -0.65$, $p = 2.3 \times 10^{-6}$; SP, $r = ^{-}0.56$, $p = 1.4 \times 10^{-3}$.

In consideration of millennium scale of deep water circulation, concentration and isotopic signature of N_2O initially existed in the water mass before subduction do not equal to the present values. Solid and broken horizontal lines in Fig. 5b respectively show the values for the surface water in the subduction region (off Greenland and off Antarctica) which is equilibrated with modern and preindustrial atmosphere[31]. The negative deviation of the SO/SIO data might indicate that relatively younger water mass in this region is affected by the mixing of modern surface water during its advection.

Production Mechanisms of N_2O in Concentration Maximum and Deep Layer

We compare the isotopocule ratio values of excess N_2O at concentration maximum and accumulated N_2O during deep water circulation with those values reported or estimated for currently known biological processes of oceanic N_2O (Fig. 4, Supplementary Table S4). The ranges of $\delta^{15}N^{bulk}$ and SP values for the N_2O maximum at most of the stations in the North Pacific and the values for deep N_2O overlap with that of N_2O produced by archaeal nitrification conducted by ammonia-oxidizing archaea (AOA)[9,10,12] (Fig. 4a). At several stations in the North Pacific and SO/SIO, SP values of N_2O at maximum concentration are larger than the range of AOA-derived N_2O, suggesting additional contribution from bacterial nitrification. In the Atlantic and at several stations in the equatorial/South Pacific and SO/SIO, N_2O maxima are accompanied by lower SP values, which indicates significant role of nitrifier-denitrification/denitrification. In contrast, $\delta^{18}O$ values obtained for both N_2O maximum and deep water N_2O are higher than that of AOA by 5–20‰ (Fig. 4b). If N_2O produced by AOA or bacterial processes is further reduced by denitrification, $\delta^{18}O$ of residual N_2O increases due to isotope fractionation[16–20]. However, the parallel increases in $\delta^{15}N^{bulk}$ and SP expected for N_2O reduction (slope of broken lines in Fig. 4) are not prominent especially for $\delta^{15}N^{bulk}$ and it is unlikely that N_2O reduction occurs in oxic seawater because N_2O reduction has been found only in anoxic environment such as ETNP or Arabian Sea[17,32]. Therefore, the discrepancy of $\delta^{18}O$ might be explained by variation of oxygen isotope effects during N_2O production by AOA. This should be tested using further laboratory studies with several species of AOA. Reported oxygen isotope fractionation during the incorporation of O_2 into N_2O is −2.2 to 13.2‰ in two marine and five soil archaeal species/isolates[9,10]. Those figures might become larger if the reaction proceeds with the equilibrium step because O-isotope exchange equilibrium fractionation between N_2O and O_2 is calculated theoretically as about 20‰ at 0–10 °C[33].

Several reports have described the dominance of AOA in nitrification in the ocean. Archaeal *amoA* gene abundance was positively correlated with potential NH_3 oxidation rate and N_2O concentration in the upper oxycline of the eastern tropical South Pacific[34]. In the oxygen minimum zone (OMZ) of the eastern tropical North Atlantic, comparable patterns of abundance and expression of archaeal *amoA* genes and N_2O co-occurred[12]. Our results suggest that AOA play a major role not only in the OMZ of tropical ocean but also in the OMZ in temperate and subarctic ocean areas and deeper waters. The average rate of N_2O production during deep water circulation estimated from the relation between N_2O concentration and circulation age of seawater is 28 f mol L^{-1} d^{-1},

which is comparable to the rate determined experimentally with pure culture of marine AOA *Nitrosopumilus maritimus* SCM1 (4.4×10^{-4}–2.4×10^{-2} f mol d^{-1} cell^{-1} under oxygen concentrations of 203–34 μmol L^{-1})[12] if one assumes cell density of AOA in deep waters as 10^4 cells L^{-1}.

Our results suggest that ubiquitous N_2O maximum in the middle layer in the North Pacific is formed by *in situ* production (mainly by AOA) rather than advection from the eastern tropical Pacific and that N_2O is also produced by AOA and accumulated during the global deep water circulation. If one simply assumes that the N_2O dissolved in the oldest deep water in NNP (34 nmol kg^{-1}) is ultimately released to the atmosphere by the circulation driven by seawater subduction in the polar regions (3×10^7 m^3 s^{-1})[35], magnitude of this deep N_2O source is estimated at up to 1 Tg N yr^{-1} compared to the estimated surface oceanic source of 3.8 Tg N yr^{-1} [1] which seems to be based on limited surface observations. This implies that change in global deep water circulation could affect concentration and isotopocule ratios of atmospheric N_2O in a millennium time scale.

Methods

Seawater samples were collected at 21 stations in the North Pacific (40–47°N, 146°E–127°W) during July–August 2007 and 4 stations in the equatorial Pacific (0°N, 160°E–158°W) in January 2003 during the MR07-04 and MR02-K06 cruises, respectively, of R/V *Mirai* (JAMSTEC, Japan) and at 8 stations in the Southern Ocean/southeastern Indian Ocean (47–65°S, 140°E) in Jan 2002 during the KH01-3 cruise of R/V *Hakuho-maru* (JAMSTEC, Japan). At each station, samples were taken at 15–28 depths in the range of 0–6000 m using 12 L Niskin bottles mounted on a conductivity-temperature-depth Rosette sampler. Each sample was collected in a 230 mL glass vial followed by addition by 1 mL saturated HgCl$_2$ solution for sterilization and by sealing with a butyl rubber stopper. Each was then preserved at 4 °C in the dark.

Concentration and isotopocule ratios of N_2O were measured using a gas chromatograph – isotope ratio mass spectrometer (GC-IRMS) equipped with a gas extraction and cryogenic concentration unit as described elsewhere[17,36]. Isotopocule ratios $^{15}R^\alpha$ ($=[^{14}N^{15}N^{16}O]/[^{14}N^{14}N^{16}O]$), $^{15}R^\beta$ ($=[^{15}N^{14}N^{16}O]/[^{14}N^{14}N^{16}O]$), and ^{18}R ($=[^{14}N^{14}N^{18}O]/[^{14}N^{14}N^{16}O]$) are expressed as delta values as defined below[37].

$$\delta X = (R - R_{\text{standard}})/R_{\text{standard}} \tag{1}$$

Therein, X denotes $^{15}N^\alpha$, $^{15}N^\beta$, or ^{18}O; R represents $^{15}R^\alpha$, $^{15}R^\beta$, or ^{18}R; R_{standard} means $[^{15}N^{14}N]/[^{14}N^{14}N]$ of atmospheric N_2 or $[H_2^{18}O]/[H_2^{16}O]$ of Vienna Standard Mean Ocean Water. In this report, we use δ value for bulk N and ^{15}N-site preference instead of $\delta^{15}N^\alpha$ and $\delta^{15}N^\beta$:

$$\delta^{15}N^{\text{bulk}} = (\delta^{15}N^\alpha + \delta^{15}N^\beta)/2, \tag{2}$$

$$SP = \delta^{15}N^\alpha - \delta^{15}N^\beta. \tag{3}$$

The typical analytical precision (1σ) is 1% for concentration, and 0.2‰, 0.4‰, and 0.9‰, respectively, for $\delta^{15}N^{\text{bulk}}$, $\delta^{18}O$, and SP.

Isotopocule ratios of excess N_2O at its maximum and those of N_2O produced *in situ* during deep water circulation were estimated by assuming the mixing of two end members.

$$C_{\text{obs}} = C_{\text{pro}} + C_{\text{atm}} \tag{4}$$

$$\delta_{\text{obs}}C_{\text{obs}} = \delta_{\text{pro}}C_{\text{pro}} + \delta_{\text{atm}}C_{\text{atm}} \tag{5}$$

Equations (4) and (5) respectively describe the mass balance of light and heavy N_2O molecules; C_{obs}, C_{pro}, C_{atm} respectively denote the observed, produced, and atmospheric equilibrium concentrations; δ_{obs}, δ_{pro}, and δ_{atm} are the respective isotopocule ratios. By eliminating C_{pro} from Eqs (4) and (5), we obtain the following:

$$\delta_{\text{pro}} = (\delta_{\text{obs}}C_{\text{obs}} - \delta_{\text{atm}}C_{\text{atm}})/(C_{\text{obs}} - C_{\text{atm}}) \tag{6}$$

The circulation age of deep seawater at each observational station was calculated from the objectively mapped circulation ^{14}C age below 1500 m in the literature[26] using "2D estimation" tool of Ocean Data View software[38].

Data Availability

Data presented in Fig. 2 are available upon request, and will be archived at http://www.godac.jamstec.go.jp/darwin/e or https://www.jodc.go.jp/jodcweb/index.html.

References

1. Ciais, P. *et al.* Carbon and other biogeochemical cycles. In *Climate Change 2013: The Physical Science Basis. Contribution of Working Group I to the Fifth Assessment Report of the Intergovernmental Panel on Climate Change* (eds Stocker, T. F. *et al.*) Chap. **6**, 465–570 (Cambridge University Press, 2013).
2. Weiss, R. F. & Price, B. A. Nitrous oxide solubility in water and seawater. *Mar. Chem.* **8**, 347–359 (1980).
3. Nevison, C. D., Weiss, R. F. & Erickson, D. J. II. Global oceanic emissions of nitrous oxide. *J. Geophys. Res.* **100**, 15809–15820 (1995).
4. Nevison, C., Butler, J. H. & Elkins, J. W. Global distribution of N_2O and the ΔN_2O-AOU yield in the subsurface ocean. *Global Biogeochem. Cycles* **17**, 1119, https://doi.org/10.1029/2003GB002068 (2003).
5. Bange, H. W. & Andreae, M. O. Nitrous oxide in the deep waters of the world's oceans. *Global Biogeochem. Cycles* **13**, 1127–1135 (1999).
6. Toyoda, S., Yoshida, N. & Koba, K. Isotopocule analysis of biologically produced nitrous oxide in various environments. *Mass Spectrom. Rev.* **36**, 135–160 (2017).
7. Yoshida, N. ^{15}N-depleted N_2O as a product of nitrification. *Nature* **335**, 528–529 (1988).

8. Frame, C. H. & Casciotti, K. L. Biogeochemical controls and isotopic signatures of nitrous oxide production by a marine ammonia-oxidizing bacterium. *Biogeosciences* **7**, 2695–2709 (2010).

9. Jung, M.-Y. *et al.* Isotopic signatures of N$_2$O produced by ammonia-oxidizing archaea from soils. *ISME J.* **8**, 1115–1125 (2014).

10. Santoro, A. E., Buchwald, C., McIlvin, M. R. & Casciotti, K. L. Isotopic signature of N$_2$O produced by marine ammonia-oxidizing archaea. *Science* **333**, 1282–1285 (2011).

11. Sutka, R. L. *et al.* Distinguishing N$_2$O production from nitrification versus denitrification based on isotopomer abundances. *Appl. Environ. Microbiol.* **72**, 638–644 (2006).

12. Löscher, C. R. *et al.* Production of oceanic nitrous oxide by ammonia-oxidizing archaea. *Biogeosciences* **9**, 2419–2429 (2012).

13. Sutka, R. L., Ostrom, N. E., Ostrom, P. H., Ghi, H. & Breznak, J. A. Erratum: Nitrogen isotopomer site preference of N$_2$O produced by Nitrosomonas europaea and Methylococcus capsulatus Bath. *Rapid Commun. Mass Spectrom.* **18**, 1411–1412 (2004).

14. Sutka, R. L., Ostrom, N. E., Ostrom, P. H., Ghi, H. & Breznak, J. A. Nitrogen isotopomer site preference of N$_2$O produced by Nitrosomonas europaea and Methylococcus capsulatus Bath. *Rapid Commun. Mass Spectrom.* **17**, 738–745 (2003).

15. Toyoda, S., Mutobe, H., Yamagishi, H., Yoshida, N. & Tanji, Y. Fractionation of N$_2$O isotopomers during production by denitrifier. *Soil Biol. Biochem.* **37**, 1535–1545 (2005).

16. Ostrom, N. E. *et al.* Isotopologue effects during N$_2$O reduction in soils and in pure cultures of denitrifiers. *J. Geophys. Res.: Biogeosci.* **112**, G02005, https://doi.org/10.1029/2006JG000287 (2007).

17. Yamagishi, H. *et al.* Role of nitrification and denitrification on the nitrous oxide cycle in the eastern tropical North Pacific and Gulf of California. *J. Geophys. Res.: Biogeosci.* **112**, G02015, https://doi.org/10.1029/2005JG000227 (2007).

18. Yoshida, N. Kinetic nitrogen isotope fractionation factors for denitrification and reduction of nitrous oxide. In *Earth, Life, and Isotopes* (eds Ohkouchi, N., Tayasu, I. & Koba, K.), 185–195 (Kyoto University Press, 2010).

19. Wahlen, M. & Yoshinari, T. Oxygen isotope ratios in N$_2$O from different environments. *Nature* **313**, 780–782 (1985).

20. Barford, C. C., Montoya, J. P., Altabet, M. A. & Mitchell, R. Steady-state nitrogen isotope effects of N$_2$ and N$_2$O production in *Paracoccus denitrificans*. *Appl. Environ. Microbiol.* **65**, 989–994 (1999).

21. Frame, C., Deal, E., Nevison, C. & Casciotti, K. L. N$_2$O production in the eastern South Atlantic: Analysis of N$_2$O stable isotopic and concentration data. *Global Biogeochem. Cycles* **28**, 1262–1278 (2014).

22. Fujii, A. *et al.* Distribution of nitrous oxide dissolved in water masses in the eastern subtropical North Pacific and its origin inferred from isotopomer analysis. *J. Oceanogr.* **69**, 147–157 (2013).

23. Toyoda, S. *et al.* Production mechanism and global budget of N$_2$O inferred from its isotopomers in the western North Pacific. *Geophys. Res. Lett.* **29**, https://doi.org/10.1029/2001GL014311 (2002).

24. Popp, B. N. *et al.* Nitrogen and oxygen isotopomeric constraints on the origins and sea-to-air flux of N$_2$O in the oligotrophic subtropical North Pacific gyre. *Global Biogeochem. Cycles* **16**, 1064, https://doi.org/10.1029/2001GB001806 (2002).

25. Charpentier, J., Farias, L., Yoshida, N., Boontanon, N. & Raimbault, P. Nitrous oxide distribution and its origin in the central and eastern South Pacific Subtropical Gyre. *Biogeosciences* **4**, 729–741 (2007).

26. Matsumoto, K. Radiocarbon-based circulation age of the world oceans. *J. Geophys. Res.* **112**, C09004, https://doi.org/10.1029/2007JC004095 (2007).

27. Hautala, S. L. The abyssal and deep circulation of the Northeast Pacific Basin. *Prog. Oceanog.* **160**, 68–82 (2018).

28. Kawabe, M. & Fujio, S. Effect of bottom slope in northeastern North Pacific on deep-water upwelling and overturning circulation. *J. Oceanogr.* **68**, 267–284 (2012).

29. Reid, J. L. On the total geostrophic circulation of the pacific ocean: flow patterns, tracers, and transports. *Prog. Oceanog.* **39**, 263–352 (1997).

30. Goreau, T. J. *et al.* Production of NO$_2^-$ and N$_2$O by nitrifying bacteria at reduced concentrations of oxygen. *Appl. Environ. Microbiol.* **40**, 526–532 (1980).

31. Prokopiou, M. *et al.* Changes in the Isotopic Signature of Atmospheric Nitrous Oxide and Its Global Average Source During the Last Three Millennia. *J. Geophys. Res.: Atmos.* **123**, 10757–710773 (2018).

32. Yoshinari, T. *et al.* Nitrogen and oxygen isotopic composition of N$_2$O from suboxic waters of the eastern tropical North Pacific and the Arabian Sea–measurement by continuous-flow isotope-ratio monitoring. *Mar. Chem.* **56**, 253–264 (1997).

33. Richet, P, Bottinga, Y. & Javoy, M. A review of hydrogen, carbon, nitrogen, oxygen, sulphur, and chlorine stable isotope fractionation among gaseous molecules. *Ann. Rev. Earth Planet. Sci.* **1977**, 65–110 (1977).

34. Peng, X. *et al.* Revisiting nitrification in the Eastern Tropical South Pacific: A focus on controls. *J. Geophys. Res.: Oceans* **121**, 1667–1684 (2016).

35. Orsi, A. H., Smethie, W. M. & Bullister, J. L. On the total input of Antarctic waters to the deep ocean: A preliminary estimate from chlorofluorocarbon measurements. *J. Geophys. Res.* **107**, 3122, https://doi.org/10.1029/2001JC000976 (2002).

36. Breider, F., Yoshikawa, C., Abe, H., Toyoda, S. & Yoshida, N. Origin and fluxes of nitrous oxide along a latitudinal transect in western North Pacific: Controls and regional significance. *Global Biogeochem. Cycles* **29**, 1014–1027 (2015).

37. Toyoda, S. & Yoshida, N. Determination of nitrogen isotopomers of nitrous oxide on a modified isotope ratio mass spectrometer. *Anal. Chem.* **71**, 4711–4718 (1999).

38. Schlitzer, R. Ocean Data View, http://odv.awi.de (2015).

Acknowledgements

Author Contributions

O.Y. and S.W. arranged and conducted seawater sampling. A.F. and H.Y. collected seawater samples and conducted N$_2$O analyses. S.T. and N.Y. made data analyses and wrote the manuscript.

Additional Information

Supplementary information accompanies this paper at https://doi.org/10.1038/s41598-019-44224-0.

Competing Interests: The authors declare no competing interests.

Publisher's note: Springer Nature remains neutral with regard to jurisdictional claims in published maps and institutional affiliations.